Acta Crystallographica Section B
**Structural Science**
ISSN 0108-7681

# Packing and polytypism in 1,10-phenanthrolin-1-ium (2-carboxyethyl)(2-carboxylatoethyl)dichlorostannate(IV)

**Weenawan Somphon,[a] Kenneth J. Haller,[a]* A. David Rae[b] and Seik Weng Ng[c]**

[a]School of Chemistry, Suranaree University of Technology, Nakhon Ratchasima 30000, Thailand, [b]Research School of Chemistry, Australian National University, Canberra ACT 0200, Australia, and [c]Institute of Postgraduate Studies and Research, University of Malaya, 50603 Kuala Lumpur, Malaysia

Correspondence e-mail: haller@sut.ac.th

Received 5 May 2005
Accepted 20 January 2006

The 1:1 adduct of $[SnCl_2(C_2H_4COOCH_3)_2]$ and 1,10-phenanthroline, $(C_{12}H_8N_2)$, which was set aside for 25 years, when recrystallized from ethanol was found to be the salt $[C_{12}H_9N_2]^+\cdot[SnCl_2(C_2H_4COO)(C_2H_4COOH)]^-$. The $Sn^{IV}$ atom in the anion has pseudo-octahedral coordination with two *cis* Cl atoms, two C atoms and two O atoms *trans* to the Cl atoms. The possibility of alternative stacking of layers perpendicular to **c*** offers an explanation for observed twinning and polytypism. An ordered, untwinned, $Z = 2$ crystal structure was determined. Pairs of adjacent anions are linked together by strong intermolecular O—H···$O^-$ hydrogen bonds, and the cation contains a strong intramolecular N—H···N hydrogen bond between its two N atoms. The protonated ring of the cation exhibits increased Lewis acidity and is linked into a network with the anions using a strong N—H···O and weak C—H···O and C—H···Cl interactions. The remaining rings of the cation form weaker C—H···O and C—H···Cl interactions. The cations stack in columns along **a** with an interplanar spacing of 3.24 Å for separations between cations inversion-related about $(1, \frac{1}{2}, \frac{1}{2})$ and 3.34 Å for separations between cations inversion-related about $(\frac{1}{2}, \frac{1}{2}, \frac{1}{2})$.

## 1. Introduction

Supramolecular synthons are important in crystal engineering and molecular networks (Desiraju, 1995, 1997; Langley *et al.*, 1998). Crystal structures with donor–acceptor groups (–OH, $–NH_2$ and –COOH) create specific strong and weak hydrogen bonding (Kuduva *et al.*, 1999, 2001; Vishweshwar *et al.*, 2002). Both the strong and the weak hydrogen bonds are a key aspect of crystalline architecture and help to predict correctly the structure and material properties of an assembly. The networks of supramolecular motifs strongly influence the local structure and ultimately the crystal packing (Liu *et al.*, 2001; Ballabh *et al.*, 2002). Previous studies of the organometallic zwitterions, cations and anions containing coordinated carboxylic acid and carboxylate groups (Braga *et al.*, 1998, 1999, 2001) show very relevant supramolecular aggregates. They show a strong hydrogen-bonded interaction when a carboxylic acid and a carboxylate cocrystallize. These important hydrogen-bonding interactions suggest the use of such species as synthons for the preparation of supramolecular aggregates.

Ng and coworkers have studied complexes between Sn and 1,10-phenanthroline and related molecules {*e.g.* $[(p\text{-}ClC_6H_4)_3SnCl\cdot H_2O\cdot o\text{-}C_{12}H_8N_2]_2$ (Ng & Das, 1996), $[Sn(C_2ClF_2O_2)(C_6H_5)_3(H_2O)]_2\cdot C_{12}H_8N_2$ (Ng, 1997), $[Sn(C_2F_3O_2)(C_6H_5)_3(H_2O)]\cdot C_{15}H_{11}N_3$ (Chee *et al.*, 2003*a*) and $[Sn_2(C_6H_5)_6(C_4H_4O_4)(H_2O)_2]\cdot 2C_{12}H_8N_2$ (Chee *et al.*, 2003*b*)}. In these

**Table 1**
Experimental details.

| | |
|---|---|
| Crystal data | |
| Chemical formula | $C_{12}H_9N_2^+ \cdot C_6H_9Cl_2O_4Sn^-$ |
| $M_r$ | 515.94 |
| Cell setting, space group | Triclinic, $P\overline{1}$ |
| Temperature (K) | 200 (1) |
| $a, b, c$ (Å) | 7.1204 (1), 12.5017 (2), 12.5780 (2) |
| $\alpha, \beta, \gamma$ (°) | 114.4242 (11), 92.5620 (11), 104.3542 (12) |
| $V$ (Å$^3$) | 973.78 (3) |
| $Z$ | 2 |
| $D_x$ (Mg m$^{-3}$) | 1.760 |
| Radiation type | Mo $K\alpha$ |
| No. of reflections for cell parameters | 25 992 |
| $\theta$ range (°) | 2.9–29.6 |
| $\mu$ (mm$^{-1}$) | 1.61 |
| Crystal form, color | Needle, transparent colorless |
| Crystal size (mm) | 0.17 × 0.14 × 0.12 |
| | |
| Data collection | |
| Diffractometer | Bruker–Nonius KappaCCD |
| Data collection method | $\varphi$ scan plus $\omega$ scans with $\kappa$ offsets |
| Absorption correction | Multi-scan (*SORTAV*; Blessing, 1995) |
| $T_{min}$ | 0.798 |
| $T_{max}$ | 0.824 |
| No. of measured, independent and observed reflections | 28 062, 5019, 4174 |
| Criterion for observed reflections | $I > 2\sigma(I)$ |
| $R_{int}$ ($P1$, before absorption correction) | 0.055 |
| $R_{int}$ ($P1$, after absorption correction) | 0.035 |
| $R_{equiv}$ [$P\overline{1}$ merge (9278 to 5019 data)] | 0.0244 |
| $\theta_{max}$ (°) | 28.7 |
| Range of $h, k, l$ | $-9 \Rightarrow h \Rightarrow 9$<br>$-16 \Rightarrow k \Rightarrow 16$<br>$-16 \Rightarrow l \Rightarrow 16$ |
| | |
| Refinement | |
| Refinement on | $F^2$ |
| $R$[all data], $wR(F^2)$, $S$ | 0.040, 0.063, 0.97 |
| $R[F^2 > 2\sigma(F^2)]$, $wR(F^2)$, $S$ | 0.029, 0.059, 1.00 |
| No. of reflections | 5019 |
| No. of parameters | 251 |
| H-atom treatment | Mixture of independent and constrained refinement |
| Weighting scheme | $w = 1/[\sigma^2(F_o^2)]$ |
| $(\Delta/\sigma)_{max}$ | 0.003 |
| $\Delta\rho_{max}$, $\Delta\rho_{min}$ (e Å$^{-3}$) | 1.31, −0.68 |

Computer programs used: *COLLECT* (Nonius, 1998), *DENZO/SCALEPACK* (Otwinowski & Minor, 1997), *SIR*97 (Altomare *et al.*, 1999), *SHELXTL* (Bruker, 1998), *ORTEP* (Burnett & Johnson, 1996; Farrugia, 1997).

structures, the organotin molecule interacts with the phenanthroline molecule indirectly through a coordinated water molecule that forms a short hydrogen bond with one of the 1,10-phenanthroline N atoms.

We report here the supramolecular structure of $[SnCl_2(C_2H_4COOH)(C_2H_4COO)]^- \cdot [C_{12}H_9N_2]^+$. When we studied this material at 200 K we obtained a data set for a perfectly ordered untwinned crystal with a unit-cell volume corresponding to $Z = 2$. However, the crystal used was obtained by cleaving a crystal that was clearly twinned because a reentrant angle defined a twin plane perpendicular to **c***. A room-temperature data set was collected by Ng (2000) for a $Z = 6$, $P\overline{1}$ structure with $a = 7.225$ (1), $b = 12.576$ (2), $c = 34.394$ (7) Å, $\alpha = 82.14$ (3), $\beta = 86.90$ (3), $\gamma = 74.84$ (3)°. The values of $a$, $b$ and $180 - \gamma$ are comparable to our values in Table 1 and suggest that these structures have the same structure for layers perpendicular to **c***. The Ng (2000) refinement was not successful ($R = 0.32$) and a strong vector in the Patterson function of $(\frac{2}{3}, \frac{1}{3}, \frac{1}{3})$ suggested pseudo-translational symmetry. However, the ratio of the height of this peak to that of the origin peak is only 0.46, suggesting that a simple displacive modulation of an ordered $Z = 2$ parent structure is unlikely. This parent structure would make no contribution to reflections with $-h + k + l \neq 3n$.

The most rational explanation of the earlier data set is that it comes from a polytype related to our structure. A suggestion of an appropriate model for the $Z = 6$ structure is provided by finding the twin plane in the $Z = 2$ structure, finding the mechanism for twinning, then using these as building principles to obtain the likely structure of the $Z = 6$ polytype. Unfortunately, we have not been able to obtain further crystals of the $Z = 6$ polytype. However, the reflection data from the $Z = 6$ polytype cannot be the result of misinterpreting the diffraction pattern of a twin of the $Z = 2$ structure (see below).

## 2. Experimental

A colorless single crystal was obtained from a large needle by cleaving to eliminate part of the crystal that was clearly twin-related because a reentrant angle defined a twin plane. A full sphere of reflection intensities were collected on a Bruker–Nonius KappaCCD diffractometer using the *COLLECT* software (Nonius, 1998). The diffractometer was equipped with a graphite-monochromated fine-focus molybdenum X-ray source, a 0.3 mm *ifg* capillary collimator and a series 600 Oxford Cryostream crystal cooler (Oxford Cryosystems, 1997) operating at 200 K. Unit-cell determination and data reduction were performed with *DENZO–SCALEPACK* (Otwinowski & Minor, 1997). Structure solution used *SIR*97 (Altomare *et al.*, 1999), and refinement used the *SHELXTL* system (Bruker, 1998). All 18 H-atom positions were located from an electron-density difference map. The coordinates and isotropic atomic displacement parameters for the NH and OH H atoms were refined, and the CH H atoms were included as idealized riding-model contributors with $U_{iso}(H) = 1.2U_{eq}(C)$. Crystal data and details of the data collection and structure refinement are summarized in Table 1. Fractional coordinates, atomic displacement parameters, mean plane calculations and other data can be found in the CIF file in the electronic archive for this paper.[1] Selected interatomic bond distances and angles are given in Tables 2 and 3. Hydrogen-bond parameters are given in Table 4.

## 3. Results and discussion

In the structure of $[SnCl_2(C_2H_4COOH)(C_2H_4COO)]^- \cdot [C_{12}H_9N_2]^+$, one H atom has transferred from a neutral Sn dicarboxylic acid complex to form a complex monoanion, $[SnCl_2(C_2H_4COOH)(C_2H_4COO)]^-$, with one –COOH and

[1] Supplementary data for this paper are available from the IUCr electronic archives (Reference: BS5018). Services for accessing these data are described at the back of the journal.

**Table 2**
Selected interatomic bond lengths (Å) and bond angles (°) for $[SnCl_2(C_2H_4COOH)(C_2H_4COO)]^-$.

| | | | |
|---|---|---|---|
| Coordination sphere | | | |
| Sn1—Cl11 | 2.4045 (6) | Cl11—Sn1—Cl12 | 96.24 (2) |
| Sn1—Cl12 | 2.4860 (6) | Cl11—Sn1—C13 | 101.30 (7) |
| Sn1—O11 | 2.5192 (18) | Cl11—Sn1—C16 | 102.65 (7) |
| Sn1—O13 | 2.3060 (17) | Cl12—Sn1—C13 | 94.67 (7) |
| Sn1—C13 | 2.127 (2) | C1l2—Sn1—C16 | 94.47 (6) |
| Sn1—C16 | 2.131 (2) | C13—Sn1—C16 | 153.22 (9) |
| Carboxylic acid $C_2H_4(COOH)$ | | Carboxylate $C_2H_4(COO^-)$ | |
| O11—Sn1—C13 | 72.78 (7) | O13—Sn1—C16 | 77.42 (7) |
| O11—Sn1—Cl11 | 172.54 (4) | O13—Sn1—Cl11 | 88.45 (5) |
| O11—Sn1—Cl12 | 88.87 (4) | O13—Sn1—C1l2 | 171.40 (4) |
| O11—Sn1—C16 | 82.30 (7) | C13—Sn1—O13 | 91.47 (8) |
| O11—Sn1—O13 | 87.19 (6) | | |
| O11—C11 | 1.232 (3) | O13—C14 | 1.272 (3) |
| C11—O12 | 1.307 (3) | C14—O14 | 1.262 (3) |
| C11—C12 | 1.502 (3) | C14—C15 | 1.515 (3) |
| C12—C13 | 1.524 (3) | C15—C16 | 1.521 (3) |
| O12—H12 | 0.72 (3) | | |
| Sn1—O11—C11 | 107.83 (14) | Sn1—O13—C14 | 112.33 (14) |
| O11—C11—O12 | 123.2 (2) | O13—C14—O14 | 122.4 (2) |
| O11—C11—C12 | 121.8 (2) | O13—C14—C15 | 118.4 (2) |
| O12—C11—C12 | 115.0 (2) | O14—C14—C15 | 119.3 (2) |
| C11—C12—C13 | 111.7 (2) | C14—C15—C16 | 111.6 (2) |
| C12—C13—Sn1 | 110.5 (2) | C15—C16—Sn1 | 108.65 (14) |
| C11—O12—H12 | 108 (3) | | |

**Table 3**
Selected interatomic bond lengths (Å) and bond angles (°) for $[C_{12}H_9N_2]^+$.

| Unprotonated ring | | Protonated ring | | Difference | Mean |
|---|---|---|---|---|---|
| C35—N34 | 1.356 (3) | C40—N41 | 1.356 (3) | 0σ | 1.356 (2) |
| C33—N34 | 1.326 (3) | C42—N41 | 1.337 (3) | +4σ | 1.332 (2) |
| C32—C33 | 1.395 (4) | C42—C43 | 1.384 (3) | −3σ | |
| C31—C32 | 1.370 (4) | C43—C44 | 1.366 (4) | −1σ | |
| C31—C36 | 1.401 (4) | C44—C39 | 1.405 (4) | +1σ | |
| C35—C36 | 1.404 (3) | C39—C40 | 1.400 (3) | −1σ | |
| | | N41—H41 | 0.79 (3) | | |
| C33—N34—C35 | 116.5 (2) | C40—N41—C42 | 122.1 (2) | +28σ | 119.3 (2) |
| C36—C35—N34 | 124.1 (2) | C39—C40—N41 | 119.5 (2) | −23σ | 121.8 (2) |
| N34—C33—C32 | 123.9 (2) | N41—C42—C43 | 120.2 (2) | −12σ | 122.1 (2) |
| C31—C36—C35 | 117.0 (2) | C44—C39—C40 | 118.2 (2) | +4σ | |
| C32—C31—C36 | 119.3 (3) | C43—C44—C39 | 120.2 (2) | +3σ | |
| C33—C32—C31 | 119.1 (3) | C42—C43—C44 | 119.6 (2) | +1σ | |
| | | C40—N41—H41 | 123 (2) | | |
| | | C42—N41—H41 | 115 (2) | | |
| Central ring | | | | | |
| C35—C40 | | | | | 1.442 (3) |
| C37—C38 | | | | | 1.346 (4) |
| C38—C39 | | | | | 1.431 (4) |
| C36—C37 | | | | | 1.431 (4) |

one $-COO^-$ group, and the 1,10-phenanthrolin-1-ium(+) monocation, $[C_{12}H_9N_2]^+$, so-called phenH$^+$ (see Fig. 1). Structures involving ionic building blocks are usually more stable than the corresponding molecular solids, including those formed exploiting strong hydrogen bonds (Lee *et al.*, 1948; Kuĺba *et al.*, 1976). The phenH$^+$ cation has two N atoms

**Table 4**
Hydrogen-bonding geometry (Å, °).

| $D$—H···$A$ | $D$—H | H···$A$ | $D$···$A$ | $D$—H···$A$ |
|---|---|---|---|---|
| Strong hydrogen bonds | | | | |
| O12—H12O···O14$^{i}$ | 0.72 (3) | 1.86 (3) | 2.579 (2) | 177 (3) |
| N41—H41N···O14$^{i}$ | 0.79 (3) | 1.91 (3) | 2.688 (2) | 166 (3) |
| N41—H41N···N34$^{ii}$ | 0.79 (3) | 2.46 (3) | 2.737 (3) | 102 (2) |
| C—H···O weak hydrogen bonds | | | | |
| C42—H42···O13$^{i}$ | 0.95 | 2.40 | 3.154 (3) | 136.0 |
| C43—H43···Cl12$^{iii}$ | 0.95 | 2.74 | 3.578 (3) | 147.8 |
| C44—H44···Cl12$^{iv}$ | 0.95 | 2.86 | 3.785 (3) | 165.4 |
| C37—H37···O13$^{v}$ | 0.95 | 2.86 | 3.458 (3) | 122.5 |
| C38—H38···O11$^{iv}$ | 0.95 | 2.70 | 3.596 (3) | 158.4 |
| C31—H31···Cl11$^{vi}$ | 0.95 | 2.95 | 3.578 (3) | 125.1 |
| C31—H31···Cl11$^{vii}$ | 0.95 | 3.04 | 3.619 (3) | 121.2 |
| C32—H32···Cl11$^{vi}$ | 0.95 | 3.18 | 3.691 (3) | 116.4 |
| C33—H33···O12$^{ii}$ | 0.95 | 2.74 | 3.377 (3) | 125.3 |

| $D$—H···$A$ | $D$···$A$ [type (*a*)] | $D$···$A$ [type (*b*)] |
|---|---|---|
| C—H···$\pi$ hydrogen bonds | | |
| C33—H33···$\pi$ | – | 3.277 (3) |
| C42—H42···$\pi$ | – | 3.309 (3) |
| N41—H41···$\pi$ | 3.235 (3) | 3.345 (8) |
| C43—H43···$\pi$ | 3.366 (3) | – |
| C44—H44···$\pi$ | 3.399 (3) | – |

Symmetry codes: (i) $1-x, -y, 1-z$; (ii) $x, y, z$; (iii) $x, y, -1+z$; (iv) $1-x, 1-y, 1-z$; (v) $x, 1+y, z$; (vi) $1-x, 1-y, 2-z$; (vii) $1+x, 1+y, z$.

only 2.74 Å apart, and protonation allows a hydrogen bond between these atoms. McBryde (1965) suggested that steric factors would usually prevent the transfer of a second proton, but subsequently neutral (phen) (Nishigaki *et al.*, 1978), monoprotonated (phenH$^+$) (Wang *et al.*, 1999*a*) and diprotonated (phenH$_2^{2+}$) (Wang *et al.*, 1999*b*) moieties have been reported.

### 3.1. The $[SnCl_2(C_2H_4COOH)(C_2H_4COO)]^-$ anion

This anion has octahedral geometry with the Cl atoms in a *cis* configuration. Each bidentate ligand is coordinated by a C and an O atom with the O atoms *trans* to Cl atoms and the C atoms *trans* to each other. The Sn—$C_{carb}$ (carb = carboxylic

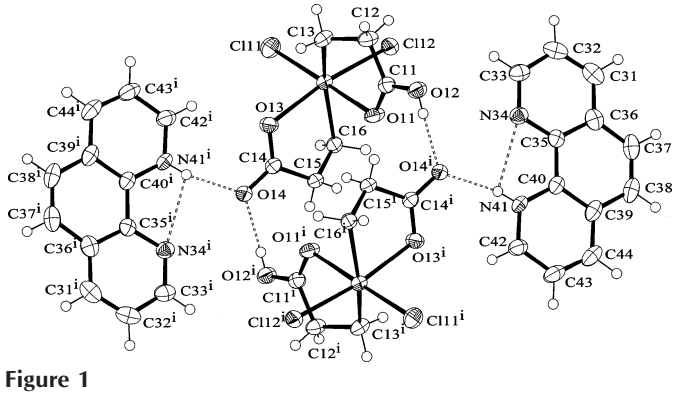


**Figure 1**
*ORTEP* (Burnett & Johnson, 1996; Farrugia, 1997) diagram of phenH$^+$ $[SnCl_2(C_2H_4COOH)(C_2H_4COO)]^-$, showing the numbering scheme and the strong hydrogen-bond interactions (50% probability displacement ellipsoids).

acid) distance of 2.127 (2) Å is not significantly shorter than the Sn—$C_{carboxy}$ (carboxy = carboxylate) distance of 2.131 (2) Å. However, the C—Sn—O (carboxylic acid) angle of 72.78 (7)° is significantly smaller than the C—Sn—O (carboxylate) angle of 77.42 (7)°. The O atom of the carboxylic acid group is more weakly bound to the Sn atom, *d*(Sn—O11) = 2.519 (2) Å, than that of the carboxylate group, *d*(Sn—O13) = 2.306 (2) Å. The difference in the tin–oxygen binding is also apparent in the coordination of the chloride anions *trans* to the O atoms. The chloride *trans* to the carboxylic acid is tightly bound, *d*(Sn—Cl11) = 2.404 (1) Å, while the chloride *trans* to the carboxylate group has *d*(Sn—Cl12) = 2.486 (1) Å. The angles of the coordination environment are distorted from ideal octahedral values because of the small bite angle of the chelate rings.

The carbon–oxygen distances, *d*(C11—O11) = 1.232 (3) Å and *d*(C11—O12) = 1.307 (3) Å, are appropriate for a carboxylic acid functional group with C11═O11 as the double bond and O12 as the OH O atom. In comparison, *d*(C14—O13) and *d*(C14—O14) are nearly equivalent at 1.272 (3) and 1.262 (3) Å, respectively. These values are consistent with the coordination geometry of a monodentate carboxylate group. The sums of the bond angles about C11 and C14 are both 360°, showing these C atoms to be $sp^2$-hybridized (see geometric parameters in Table 2).

### 3.2. The 1,10-phenanthrolin-1-ium cation

One of the phen N atoms is protonated while the other N atom is not. The *d*(N41—H41) = 0.79 (3) Å value is comparable to literature values of 0.78 Å (Cesario *et al.*, 1986), and 0.76 and 0.74 Å (Krishnakumar *et al.*, 1996). Protonation of N41 causes the C—N—C angle to increase [122.1 (2)° in the protonated ring *versus* 116.5 (2)° in the unprotonated ring], in agreement with literature values of 123.2 (3)° for the protonated ring and 116.4 (3)° for the unprotonated ring (Bakshi *et al.*, 1996*a*), and of 121.9 (7)° for the protonated ring and 115.2 (8)° for the unprotonated ring (Bakshi *et al.*, 1996*b*). The bond distances about the N atoms do not differ significantly between the protonated ring and the unprotonated ring (see Table 3). This angle increase at the N atom of $phenH^+$ agrees with a previously reported structure (Wang *et al.*, 1999*a*). In the case of neutral (Nishigaki *et al.*, 1978) and $phenH_2^{2+}$ (Wang *et al.*, 1999*b*) it was found that the bond angles are similar but the angles in $phenH_2^{2+}$, 122.7°, are greater than for neutral phen, 117.8°. Thus, while it can be said that the $NH^+$ protonated bond is less repulsive to the N—C bonds than the N lone pair, the increased effect on the angle in the unprotonated ring of the $phenH^+$ cation is from the strong intramolecular hydrogen bond. It should be noted that a 1:1 disorder of $phenH^+$ would produce an average geometry with equal N environments. The mean values of disorder-related distances and angles are given in Table 3.

### 3.3. Supramolecular structure and hydrogen bonding

**3.3.1. The strong anion–anion interactions**. The monoanions are held together by strong intermolecular hydrogen bonds (see Fig. 1 and Table 4). The carboxylate O14 atom and the H atom of O12 of an adjacent monoanion complex exhibit an O14···O12 distance of 2.579 (2) Å. This can be compared with the distances of 2.570 Å between monoanions in the structure of $[Cr(\eta^6\text{-}C_6H_6)_2][\{(Fe(\eta^5\text{-}C_5H_4COOH)(\eta^5\text{-}C_5H_4COO)][Fe(\eta^5\text{-}C_5H_4COOH)_2]_{0.5}\}$ (Braga *et al.*, 1998).

**3.3.2. The strong anion–cation interactions**. The crystal structure is composed of layers of anions, $[SnCl_2(C_2H_4CO_2H)(C_2H_4CO_2)]^-$, and cations, $phenH^+$, held together by strong N—H···O hydrogen bonds (see Fig. 1). The O14 atom of the carboxylate ligand participates in a bifurcated hydrogen bond involving the H atoms of N41 of the adjacent $phenH^+$ cation, with an N41···O14 distance of 2.688 (2) Å.

**3.3.3. The intramolecular cation interactions**. There is a strong intramolecular hydrogen-bond interaction between the N atom in the protonated ring and the N atom of the unprotonated ring, with an N41···N34 distance of 2.737 (3) Å. This interaction is part of the bifurcated hydrogen bonding mentioned above. Our values in Table 3 may be compared with those of Bakshi *et al.* (1996*b*) for the corresponding geometry: *d*(N···N) = 2.722 (9) Å, *d*(H···N) = 2.39 Å and the N—H···N angle is 98°.

**3.3.4. The weak anion–cation interactions**. These weaker interactions can play an important role in structure stabilization. The interactions are shown in Fig. 2. Values are given in Table 4. The hydrogen bond involving C42 of the protonated ring is a shorter distance, *d*[C42···O13] = 3.154 (3) Å, than *d*(C33···O12) = 3.377 (3) Å involving the other nitrogen-containing ring. Distances involving the remaining ring are *d*(C37···O13) = 3.458 (3) Å and *d*(C38···O11) = 3.596 (3) Å. The increased Lewis acidity of the protonated ring can be seen in this shorter C···O contact. There are also weak C—H···Cl hydrogen bonds. Average C···Cl distances are similar for the protonated and unprotonated rings.

**3.3.5. The weak cation–cation ($phenH^+$···$phenH^+$) stacking pairs**. The $phenH^+$ ions stack face-to-face and are held together by weak intermolecular interactions. They stack in columns along **a** with adjacent cations related by inversion centers. The inversion at (*a*) ($\frac{1}{2}$, $\frac{1}{2}$, $\frac{1}{2}$) is not equivalent to the

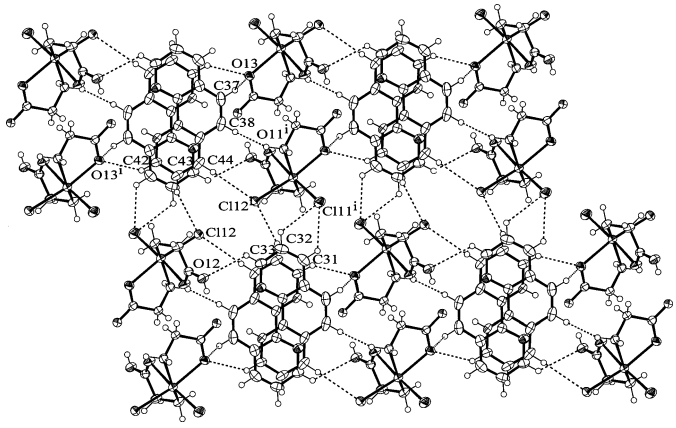


**Figure 2**
*ORTEP* (Burnett & Johnson, 1996; Farrugia, 1997) diagram showing the weak anion–cation hydrogen-bond interactions as dashed lines.

inversion at (*b*) (1, $\frac{1}{2}$, $\frac{1}{2}$), but centers separated by **a** are equivalent. The center of the C35—C40 bond is shifted 0.94 Å laterally in case (*a*) and 2.29 Å in case (*b*). In case (*a*) the cations are held together by one stronger N—H$\cdots\pi$ and two weaker C—H$\cdots\pi$ interactions and their inversion-related interactions (see Table 4). In case (*b*) there are the same number and type of interactions but the overlap is optimal (Fig. 3*a versus* Fig. 3*b*). As the (*a*) and (*b*) pair alternate along the column the interplanar spacing also alternates with the longer 3.34 Å spacing about ($\frac{1}{2}$, $\frac{1}{2}$, $\frac{1}{2}$) and the shorter 3.24 Å spacing about (1, $\frac{1}{2}$, $\frac{1}{2}$). The shorter spacing indicates a stronger interaction for the optimally overlapped case.

The combination of the strong hydrogen bonds, the cation–cation stacking interactions, and the other weak non-covalent bonding interactions, except the C—H$\cdots$Cl interactions, leads to the layer structure illustrated as a projection down **c*** in Fig. 4. The only interlayer interactions are the weak C—H$\cdots$Cl interactions already noted (Fig. 2), which in Fig. 5, showing a projection down **a**, make an interface between parallel layers at $z$ = 1.

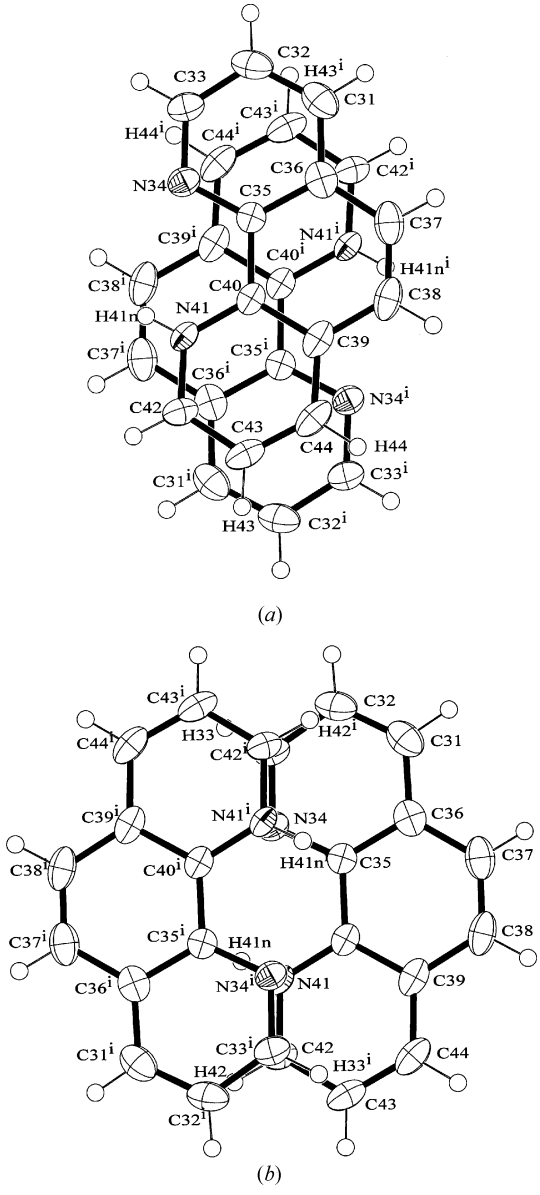


**Figure 3**
Illustration of the phenH$^+\cdots$phenH$^+$ stacked pairs projected onto the phenH$^+$ planes. (*a*) *a*-type about ($\frac{1}{2}$, $\frac{1}{2}$, $\frac{1}{2}$); (*b*) *b*-type about (1, $\frac{1}{2}$, $\frac{1}{2}$) (see text).

### 3.4. The possible packing of layers perpendicular to c*

An estimate of the 200 K unit cell for the $Z$ = 6 polytype can be obtained from the 200 K unit cell for the $Z$ = 2 polytype by the transformation $\mathbf{a}' = -\mathbf{a}$, $\mathbf{b}' = \mathbf{b}$, $\mathbf{c}' = -\mathbf{a} - \mathbf{b} - 3\mathbf{c}$ to give $a'$ = 7.120, $b'$ = 12.502, $c'$ = 34.243 Å, $\alpha'$ = 81.83, $\beta'$ = 86.09, $\gamma'$ = 75.65°. This can be compared with the room-temperature cell by Ng (2000) of $a$ = 7.225 (1), $b$ = 12.576 (2), $c$ = 34.394 (7) Å, $\alpha$ = 82.14 (3), $\beta$ = 86.90 (3), $\gamma$ = 74.84 (3)°. This $Z$ = 6 cell is a change of reduced cell after simply trebling the $c$-axis repeat of the $Z$ = 2 cell. Thus, $\mathbf{c} = (-\mathbf{a}' + \mathbf{b}' + \mathbf{c}')/3$ and this vector corresponds to the largest peak in the Patterson map of the $Z$ = 6 polytype. However, the ratio of the height of this peak to the origin peak is only 0.46. A twinning of the $Z$ = 2 structure by a twofold screw axis parallel to **c*** creates twin-related reflections indexable relative to the reciprocal axes of the reference cell as $-h\mathbf{a}^* - k\mathbf{b}^* + l''\mathbf{c}^*$, where $l'' = l + h2|a^*/c^*|\cos\alpha^* + k2|b^*/c^*|\cos\beta^* = l + 0.5542h + 0.9102k$ and this cannot be an explanation of the $Z$ = 6 cell.

A polytype that would triple the cell volume has the layer sequence *ABAABAABA*$\cdots$, where *B* layers are twofold

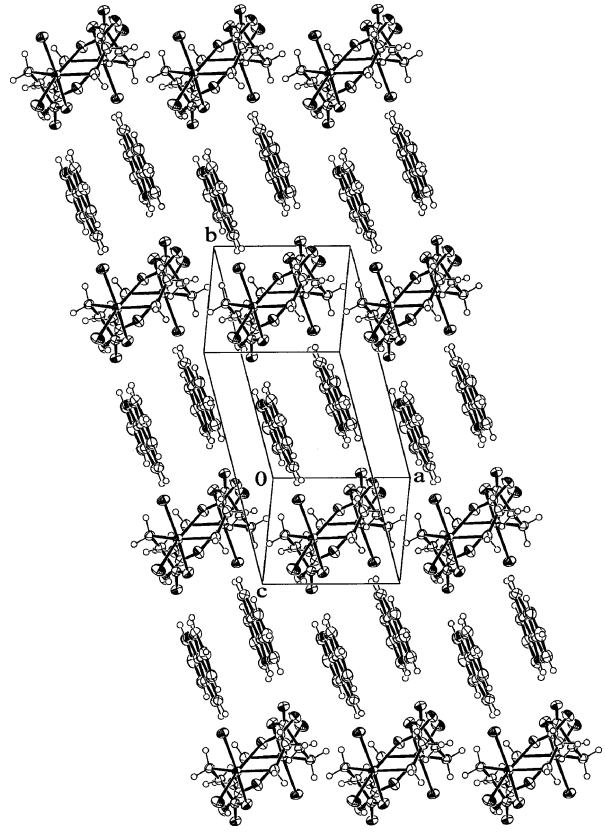


**Figure 4**
The contents of a single layer projected down **c***.

rotated about **c*** versions of *A* layers, with $A \Rightarrow A$ corresponding to the translational repeat **c** and $A \Rightarrow B \Rightarrow A$ fortuitously corresponding to the translational repeat 2**c**, modulo **a** and **b**. This can be achieved by choosing the location of layer *B* and only having true inversion centers in the middle of layer *B* and between adjacent layers *A*. The relationship between adjacent layers *A* and *B* is now a pseudo-twofold screw parallel to **c***.

In the $Z = 6$ structure corresponding pseudo-inversion centers of layers of type *A* at **c**/2 and 5**c**/2 + *m***a** + *n***b** are pseudo-screw-related to a layer of type *B* with its corresponding center of inversion at 3**c**/2 + *m***a**/2 + *n***b**/2, where *m* and *n* are integers to be determined and **a**, **b**, **c** refer to the $Z = 2$ structure. As a consequence, the pseudo-screw axis relating the layer at **c**/2 to that at 3**c**/2 passes through the point **c** + *m***a**/4 + *n***b**/4. Figs. 4–6 suggest *m* is odd and *n* is even if coincident origins are used for the inversion-related adjacent layers of type *A* at **c**/2. Thus, a real inversion at **a**/2 + **b** + 3**c**/2 is pseudo-screw-related to the pseudo-inversion at **c**/2.

The projection of the vector **c** onto the plane of **a** and **b** (the plane of the layers in Fig. 4) is given by $-|a^*/c^*|\cos\beta^*\,\mathbf{a} - |b^*/c^*|\cos\alpha^*\,\mathbf{b} = -0.2771\mathbf{a} - 0.4551\mathbf{b}$. The interlayer interface at $z = 1$ shown in Fig. 5 suggests an alternative interlayer relationship between adjacent layers as a mechanism for twinning (identification of this interface as the twin plane) or polytypism (a selection between options for the packing of layers, the sequence choice identifying the polytype). A pseudo-twofold screw operation could relate adjacent layers, the axis passing through the point $(x, \frac{1}{2}, 1)$ where *x* is indeterminable from Fig. 5. Fig. 6 shows a projection down **b** and suggests that the pseudo-twofold screw axis passes through the point $(\frac{1}{4}, y, 1)$, where *y* is indeterminable from Fig. 6. A consistent description of this pseudo-screw axis is that it passes through $(\frac{1}{4}, \frac{1}{2}, 1)$.

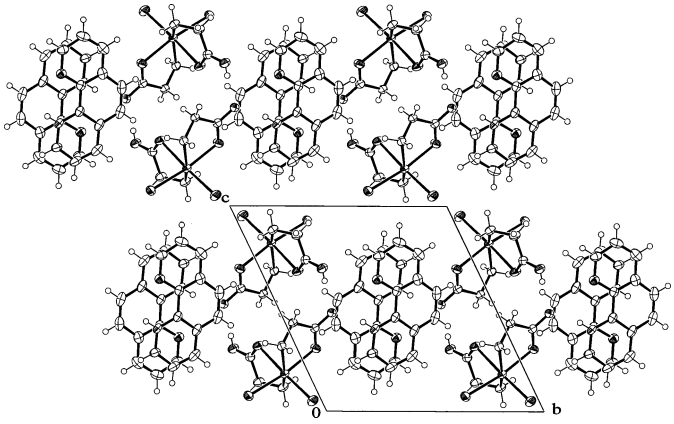


**Figure 5**
Packing diagram projected down **a**.

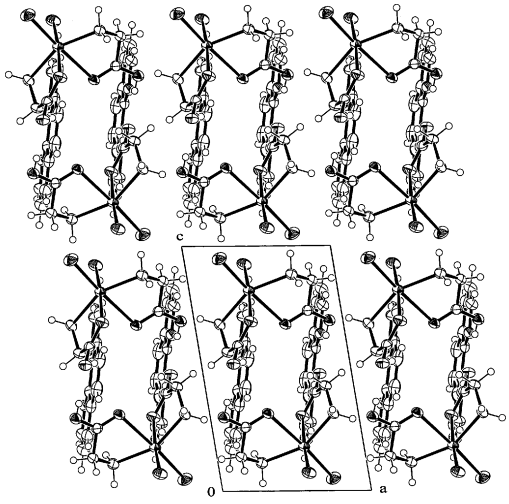


**Figure 6**
Packing diagram projected down **b**.

We have thus created a believable polytype structure from an accurately determined structure. In the process we have found a twin-disorder mechanism. If stacking faults exist, the extra translation by **c** reduces the scale of reflections with $-h' + k' + l' \neq 3n$ and increases the size of the Patterson peak at $(\frac{2}{3}, \frac{1}{3}, \frac{1}{3})$. The possibility of different polytypes in the one crystal (Rae & Willis, 2003) is known and the quality of the data previously collected for the $Z = 6$ polytype was not very good. Unfortunately, we have not been able to reobtain crystals of the $Z = 6$ polytype to obtain a better data set collected using area-detector technology. It should be noted that interfacially twinned crystals are the general rule and these can be identified by the existence of a reentrant angle in the crystal form. If twinning was present in the crystal of the $Z = 6$ modification studied this could explain the reduced quality of the data collected. The twin would cause spot splitting of twin-related reflections along **c**′* in reciprocal space.

WS thanks the Royal Golden Jubilee PhD Program, Thailand Research Fund, for support of her graduate studies under grant No. PHD/0127/2542 and Basic Research Grant No. BGJ/22/2544.

## References

Altomare, A., Burla, M. C., Camalli, M., Cascarano, G. L., Giacovazzo, C., Guagliardi, A., Moliterni, A. G. G., Polidori, G. & Spagna, R. (1999). *J. Appl. Cryst.* **32**, 115–119.
Bakshi, P. K., Cameron, T. S. & Knop, O. (1996*a*). *Can. J. Chem.* **74**, 201–220.
Bakshi, P. K., Cameron, T. S. & Knop, O. (1996*b*). *Can. J. Chem.* **74**, 559–573.
Ballabh, A., Trivedi, D. R., Dastidar, P. & Suresh, E. (2002). *Cryst. Eng. Commun.* **4**, 135–142.
Blessing, R. (1995). *Acta Cryst.* A**51**, 33–38.
Braga, D., Maini, L. & Grepioni, F. (1998). *Angew. Chem. Int. Ed. Engl.* **37**, 2240–2242.
Braga, D., Maini, L., Grepioni, F., Elschenbroich, C., Paganelli, F. & Schiemann, O. (2001). *Organometallics*, **20**, 1875–1881.
Braga, D., Maini, L., Polito, M. & Grepioni, F. (1999). *Organometallics*, **18**, 2577–2579.
Bruker (1998). *SHELXTL.* Version 5.1. Bruker AXS Inc., Madison, Wisconsin, USA.
Burnett, M. N. & Johnson, C. K. (1996). *ORTEPIII.* Report ORNL-6895. Oak Ridge National Laboratory, Tennessee, USA.
Cesario, M., Dietrich, C. O., Edel, A., Guilhem, J., Kintzinger, J. P., Pascard, C. & Sauvage, J. P. (1986). *J. Am. Chem. Soc.* **108**, 6250–6254.

Chee, C. F., Lo, K. M. & Ng, S. W. (2003*a*). *Acta Cryst.* E**59**, m36–m37.
Chee, C. F., Lo, K. M. & Ng, S. W. (2003*b*). *Acta Cryst.* E**59**, m642–m643.
Desiraju, G. R. (1995). *Angew. Chem. Int. Ed. Engl.* **34**, 2311–2327.
Desiraju, G. R. (1997). *J. Chem. Soc. Chem. Commun.* pp. 1475–1482.
Farrugia, L. J. (1997). *J. Appl. Cryst.* **30**, 565.
Krishnakumar, R., Aravamudan, G., Udupa, M. R., Seshasayee, M. & Hamor, T. A. (1996). *J. Chem. Soc. Dalton Trans.* pp. 2253–2259.
Kuduva, S. S., Bläser, D., Boese, R. & Desiraju, G. R. (2001). *J. Org. Chem.* **66**, 1621–1626.
Kuduva, S. S., Craig, D. C., Nangia, A. & Desiraju, G. R. (1999). *J. Am. Chem. Soc.* **121**, 1936–1944.
Kuĺba, F. Y., Makashev, Y. A. & Fedyaev, N. I. (1976). *Russ. J. Inorg. Chem.* **21**, 1178–1185.
Langley, P. J., Hulliger, J., Thaimattam, R. & Desiraju, G. R. (1998). *New J. Chem.* pp. 1307–1309.
Lee, T. S., Kolthoff, I. M. & Leussing, D. L. (1948). *J. Am. Chem. Soc.* **70**, 2348–2352.
Liu, R., Mok, K.-F. & Valiyaveettil, S. (2001). *New J. Chem.* pp. 890–892.
McBryde, W. A. E. (1965). *Can. J. Chem.* **43**, 3472–3476.
Ng, S. W. (1997). *Acta Cryst.* C**53**, 1059–1061.
Ng, S. W. (2000). Unpublished results. University of Malaya, Kuala Lumpur, Malaysia.
Ng, S. W. & Das, V. G. K. (1996). *J. Organomet. Chem.* **513**, 105–108.
Nishigaki, S., Yoshioka, H. & Nakatsu, K. (1978). *Acta Cryst.* B**34**, 875–879.
Nonius (1998). *Collect.* Nonius BV, Delft, The Netherlands.
Otwinowski, Z. & Minor, W. (1997). *Methods Enzymol.* **276**, 307–326.
Oxford Cryosystems (1997). *600 Series Cryostream Cooler Operation and Instruction Guide.* Oxford Cryosystems, Oxford, UK.
Rae, A. D. & Willis, A. C. (2003). *Z. Kristallogr.* **218**, 295–296.
Vishweshwar, P., Nangia, A. & Lynch, V. M. (2002). *J. Org. Chem.* **67**, 556–565.
Wang, Y.-Q., Wang, Z.-M., Liao, C.-S. & Yan, C.-H. (1999*a*). *Acta Cryst.* C**55**, 1503–1506.
Wang, Y.-Q., Wang, Z.-M., Liao, C.-S. & Yan, C.-H. (1999*b*). *Acta Cryst.* C**55**, 1506–1508.